


RESEARCH

Open Access



Arcuate AgRP, but not POMC neurons, modulate paraventricular CRF synthesis and release in response to fasting

Alan Carlos Alves Fernandes^{1†}, Franciane Pereira de Oliveira^{6†}, Gimena Fernandez⁵, Luane da Guia Vieira¹, Cristiane Gugelmin Rosa¹, Taís do Nascimento¹, Suzelei de Castro França¹, Jose Donato Jr.³, Kristen R. Vella⁴, Jose Antunes-Rodrigues², André Mecawi⁶, Mario Perello⁵, Lucila Leico Kagohara Elias² and Rodrigo Rorato^{1,6*} 

Abstract

Background: The activation of the hypothalamic–pituitary–adrenal (HPA) axis is essential for metabolic adaptation in response to fasting. However, the neurocircuitry connecting changes in the peripheral energy stores to the activity of hypothalamic paraventricular corticotrophin-releasing factor (CRF^{PVN}) neurons, the master controller of the HPA axis activity, is not completely understood. Our main goal was to determine if hypothalamic arcuate nucleus (ARC) POMC and AgRP neurons can communicate fasting-induced changes in peripheral energy stores, associated to a fall in plasma leptin levels, to CRF^{PVN} neurons to modulate the HPA axis activity in mice.

Results: We observed increased plasma corticosterone levels associate with increased CRF^{PVN} mRNA expression and increased CRF^{PVN} neuronal activity in 36 h fasted mice. These responses were associated with a fall in plasma leptin levels and changes in the mRNA expression of *AgRP* and *Pomc* in the ARC. Fasting-induced decrease in plasma leptin partially modulated these responses through a change in the activity of ARC neurons. The chemogenetic activation of POMC^{ARC} by DREADDs did not affect fasting-induced activation of the HPA axis. DREADDs inhibition of AgRP^{ARC} neurons reduced the content of CRF^{PVN} and increased its accumulation in the median eminence but had no effect on corticosterone secretion induced by fasting.

Conclusion: Our data indicate that AgRP^{ARC} neurons are part of the neurocircuitry involved in the coupling of PVN^{CRF} activity to changes in peripheral energy stores induced by prolonged fasting.

Keywords: HPA axis, CRF, Fasting, AgRP, DREADD

Background

The hypothalamic–pituitary–adrenal (HPA) axis consists of hypophysiotropic corticotropin-releasing factor (CRF) neurons, localized in the medial parvocellular

subdivision of the PVN (CRF^{PVN}), that control the synthesis and secretion of ACTH from the anterior pituitary that in turn modulates the glucocorticoid secretion (e.g., corticosterone in rodents) from the adrenal gland [1]. As the major HPA axis regulator, CRF^{PVN} neurons are responsible for orchestrating endocrine, autonomic and behavioral responses to stress [2–4].

Increased HPA axis activity is observed in response to different kinds of clinical metabolic disorders, such as obesity, metabolic syndrome, type 1 and 2 diabetes, and HIV-related lipodystrophy [5–7]. Despite the differences

[†]Alan Carlos Alves Fernandes and Franciane Pereira de Oliveira contributed equally to this work

*Correspondence: rorato@unifesp.br

¹ Department of Biotechnology, University of Ribeirão Preto, Ribeirão Preto, SP 14096-900, Brazil

Full list of author information is available at the end of the article



in the pathogenesis of these conditions, it has been suggested that changes in peripheral energy stores or the inability of the organism to sense them, underlie the changes in the HPA axis activity [8]. Reinforcing the coupling of the HPA axis with changes in peripheral energy stores, it was demonstrated that leptin administration reduces corticosterone in hypoleptinemic type 1 diabetic animals [9–11] and restores fasting-increased plasma corticosterone levels in mice [9].

The central nervous system (CNS) is considered the critical site for leptin's actions on food consumption and energy expenditure [12]. Leptin receptor (LepR) is not expressed in CRF^{PVN} neurons [13] but it is highly expressed in brain sites sensitive to changes in peripheral energy stores, such as the hypothalamic arcuate nucleus (ARC), where LepR colocalizes with a subset of proopiomelanocortin (POMC) or agouti-related protein (AgRP) neurons (POMC^{ARC} or AgRP^{ARC} neurons, respectively) [14]. In the ARC, POMC is predominantly cleaved to alpha-melanocyte stimulating hormone (α -MSH) that negatively modulates the energy homeostasis [10]. On the other hand, the activation of AgRP^{ARC} neurons, which also produce neuropeptide Y (NPY) and GABA, increases food intake and reduces energy expenditure [10]. Additionally, pharmacological studies have demonstrated that α -MSH, AgRP and NPY signaling can modulate the HPA axis activity [15, 16]. The ARC neurons are both directly and indirectly connected to the PVN [17, 18]. However, in addition to the ARC, these neuropeptides/neurotransmitters are also expressed in other brain nuclei [19–21].

Therefore, in the present study we aimed to determine if POMC^{ARC} and/or AgRP^{ARC} neurons can communicate fasting-induced changes in peripheral energy stores to CRF^{PVN} neurons.

Results

Fasting activates the HPA axis

Initially, the effects of 24 h and 36 h fasting were compared. Both fasting periods reduced the body weight, plasma leptin and blood glucose levels, and increased plasma corticosterone concentration; however, only 36 h fasting increased mRNA expression of *Crf* in the PVN and *Agrp* and *Npy* in the ARC, as compared to 24 h fasting (Additional file 2: Fig. S2). Therefore, the additional studies were performed in 36 h-fasted animals.

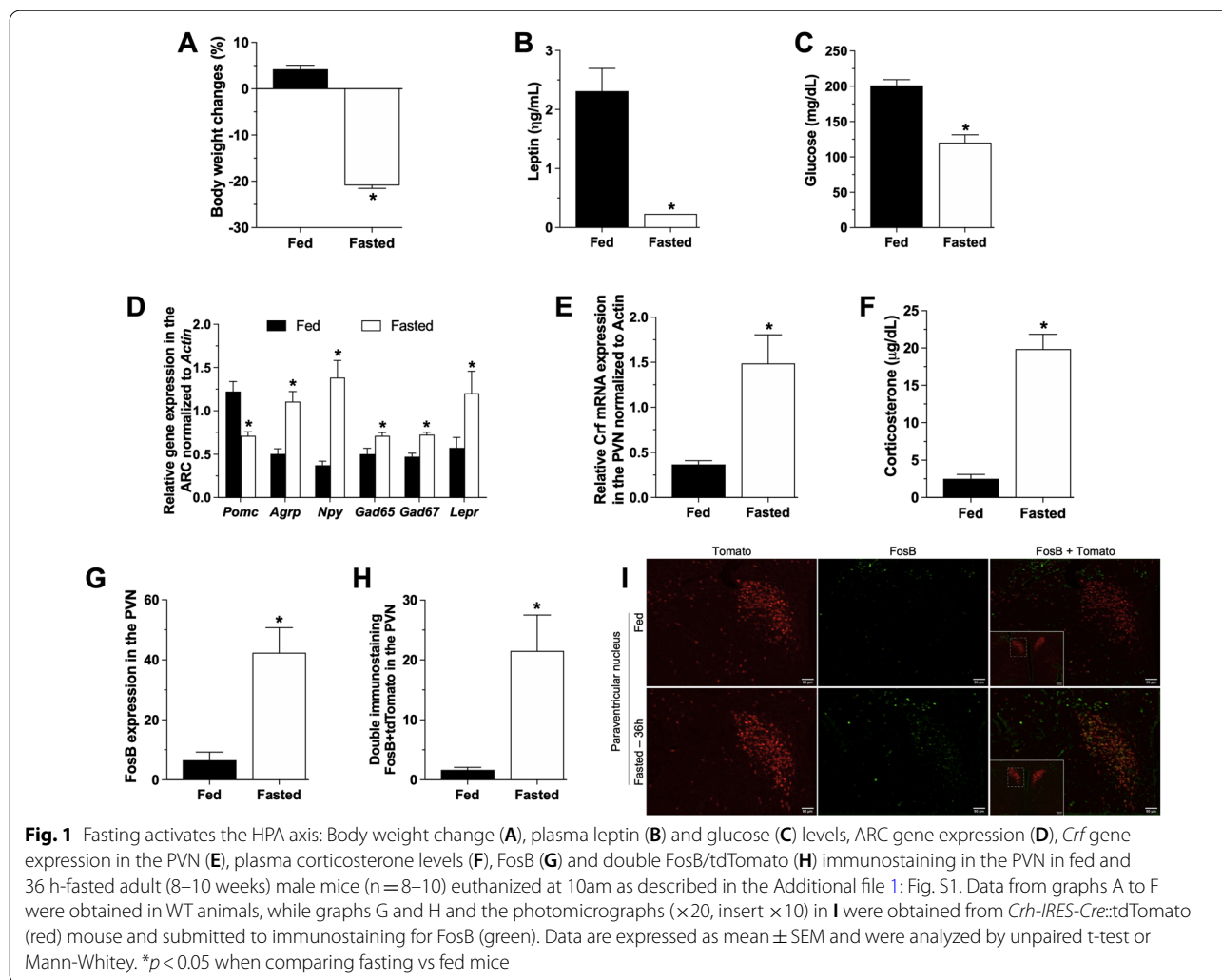
We observed body weight loss (Fig. 1A, fed=4.2±0.8%BWC and fasted=-20.9±0.6%BWC, Mann–Whitney test, $p=0.001$) associated with increased plasma corticosterone levels (Fig. 1F, fed=2.5±0.5 μ g/dL and fasted=19.8±1.9 μ g/dL, unpaired t test, $p<0.0001$), mRNA expression of *Crf* in the PVN (Fig. 1E, fed=0.3±0.0 AU and fasted=1.4±0.3 AU, unpaired t test, $p=0.01$) and

increased CRF^{PVN} neuronal activity (Fig. 1H, fed=1.7±0.4 FosB+tdTomato and fasted=21.5±6 FosB+tdTomato, unpaired t test, $p=0.001$) in 36 h fasted mice compared to fed mice. As expected, we also observed reduced plasma glucose (Fig. 1C, fed=201±8.1 mg/dL and fasted=120±11.1 mg/dL, unpaired t test, $p<0.0001$) and leptin (Fig. 1B, fed=2.3±0.3 ng/mL and fasted=0.2±0.0 ng/mL, unpaired t test, $p=0.002$) levels in 36 h fasted mice. Additionally, in the ARC of 36 h-fasted animals, we observed increased mRNA expression of *Agrp* (fed=0.5±0.3 AU and fasted=1.1±0.1 AU, unpaired t test, $p=0.003$), *Npy* (fed=0.3±0.0 AU and fasted=1.3±0.1 AU, unpaired t test, $p=0.003$), *Gad65* (fed=0.5±0.0 AU and fasted=0.7±0.0 AU, unpaired t test, $p=0.02$), *Gad67* (fed=0.4±0.0 AU and fasted=0.7±0.0 AU, unpaired t test, $p=0.0008$) and *Lepr* (fed=0.6±0.1 AU and fasted=1.2±0.2 AU, Mann–Whitney test, $p=0.03$), and decreased *Pomc* mRNA expression (fed=1.2±0.1 AU and fasted=0.7±0.0 AU, unpaired t test, $p=0.003$) (Fig. 1D).

Leptin treatment prevents HPA axis activation under fasting

Leptin treatment robustly increased plasma leptin levels (Fig. 2B, fasted+saline=0.23±0.0 ng/mL, fasted+0.5 leptin=29.9±8.2 ng/mL and fasted+1.0 leptin=72.7±17 ng/mL, Kruskal–Wallis test, $p<0.05$) but had no effect on fasting-induced body weight loss (Fig. 2A, fasted+saline=-22.5±0.3%BWC, fasted+0.5 leptin=-22.8±0.5%BWC and fasted+1.0 leptin=-21.5±0.9%BWC, Kruskal–Wallis test, $p=0.003$). Additionally, leptin treatment reduced fasting-induced corticosterone secretion (Fig. 2F, fasted+saline=19.4±1.7 μ g/dL, fasted+0.5 leptin=8.1±1.8 μ g/dL and fasted+1.0 leptin=7.8±1.2 μ g/dL, one-way ANOVA followed by post hoc Tukey's multiple comparison, $p<0.001$), associated with reduction of *Crf* mRNA expression (Fig. 2E, fasted+saline=1.3±0.1 AU, fasted+0.5 leptin=0.6±0.1 AU and fasted+1.0 leptin=0.7±0.1 AU, one-way ANOVA followed by post hoc Tukey's multiple comparison, $p=0.002$). Leptin treatment (1 μ g/g) also reduced the fasting-induced FosB expression in CRF^{PVN} neurons (Fig. 2H, fasted+saline=35.2±12 FosB+tdTomato and fasted+leptin 1 μ g/g=9±1.8 FosB+tdTomato, unpaired t test, $p=0.057$). We also observed reduced plasma glucose levels (fasted+saline=102±6.1 mg/dL, fasted+0.5 leptin=66.3±3.3 mg/dL and fasted+1.0 leptin=67.8±3.4 mg/dL, Kruskal–Wallis test, $p<0.001$) in leptin-treated fasted animals (Fig. 2C).

We also observed reduced plasma glucose levels (fasted+saline=102±6.1 mg/dL, fasted+0.5 leptin=66.3±3.3 mg/dL and fasted+1.0 leptin=67.8±3.4 mg/dL, Kruskal–Wallis test, $p<0.001$) in leptin-treated fasted



animals (Fig. 2C). Administration of leptin to fasted animals increased the mRNA expression of *Pomc* (fasted + saline = 0.9 ± 0.1 AU, fasted + 0.5 leptin = 1.4 ± 0.1 AU and fasted + 1.0 leptin = 1.4 ± 0.2 AU, one-way ANOVA followed by post hoc Tukey’s multiple comparison, *p* < 0.05) and reduced *Npy* (fasted + saline = 1.9 ± 0.2 AU, fasted + 0.5 leptin = 1.7 ± 0.2 AU and fasted + 1.0 leptin = 1.1 ± 0.0 AU, one-way ANOVA followed by post hoc Tukey’s multiple comparison, *p* < 0.05) and *Gad67* (fasted + saline = 1.3 ± 0.0 AU, fasted + 0.5 leptin = 0.9 ± 0.0 AU and fasted + 1.0 leptin = 0.9 ± 0.0 AU, one-way ANOVA followed by post hoc Tukey’s multiple comparison, *p* < 0.05) in the ARC (Fig. 2D).

Chemogenetic activation of POMC^{ARC} neurons do not affect fasting-induced HPA axis activation

Bilateral AAV-DIO-hM3DGq-mCherry and AAV-DIO-mCherry injections in the ARC were equally efficient in targeting POMC^{ARC} neurons (Fig. 3A, mCherry=89.2±6.8 mCherry+ cells and hM3DGq=72.3±6.2 mCherry+ cells,

unpaired *t* test, *p*=0.1). We confirmed the chemogenetic activation of POMC^{ARC} neurons by the increased FosB + mCherry expression in the ARC (mCherry=1.0±0.6 FosB+mCherry cells and hM3DGq=28.6±3.7 FosB+mCherry cells, Mann–Whitney test, *p*=0.002) of *Pomc-Cre* animals treated with CNO (Fig. 3B,C). Surprisingly, activation of POMC^{ARC} reduced fasting-induced body weight loss (Fig. 3D, mCherry+saline= -19.2±0.6%BWC, mCherry+CNO= -18.8±1.0%BWC, hM3DGq+saline=-19.3±0.6%BWC and hM3DGq+CNO= -15.8±0.3%BWC, two-way ANOVA followed by post hoc Tukey’s multiple comparison, * and #*p*=0.01) and this response was associated with increased plasma leptin (Fig. 3E, mCherry=0.2±0.0 ng/mL and hM3DGq=0.9±0.3 ng/mL, Mann–Whitney test, *p*=0.01) and glucose levels (Fig. 3F, mCherry=79.3±7.1 mg/dL and hM3DGq=176.6±24.8 mg/dL, Mann–Whitney test, *p*=0.001).

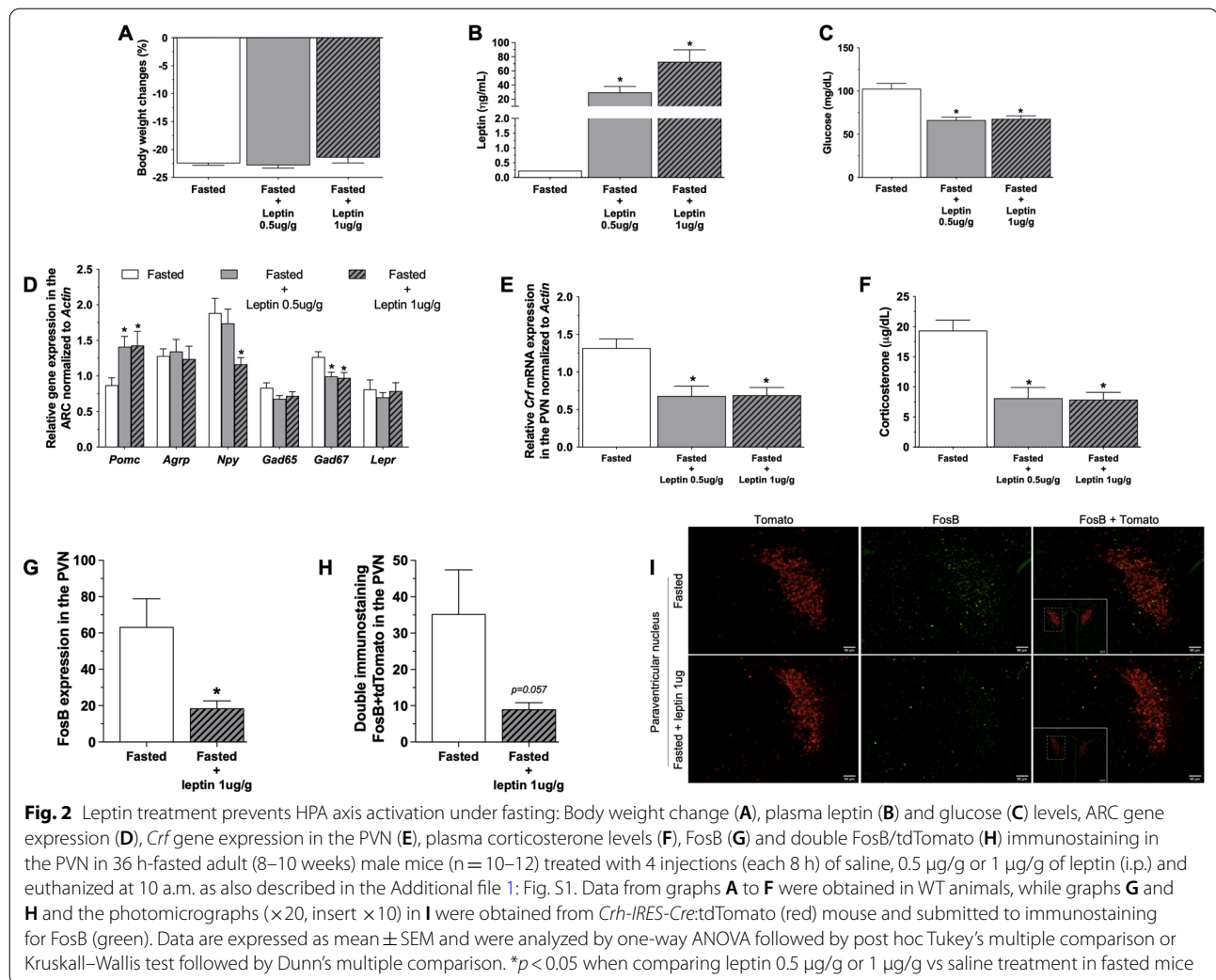


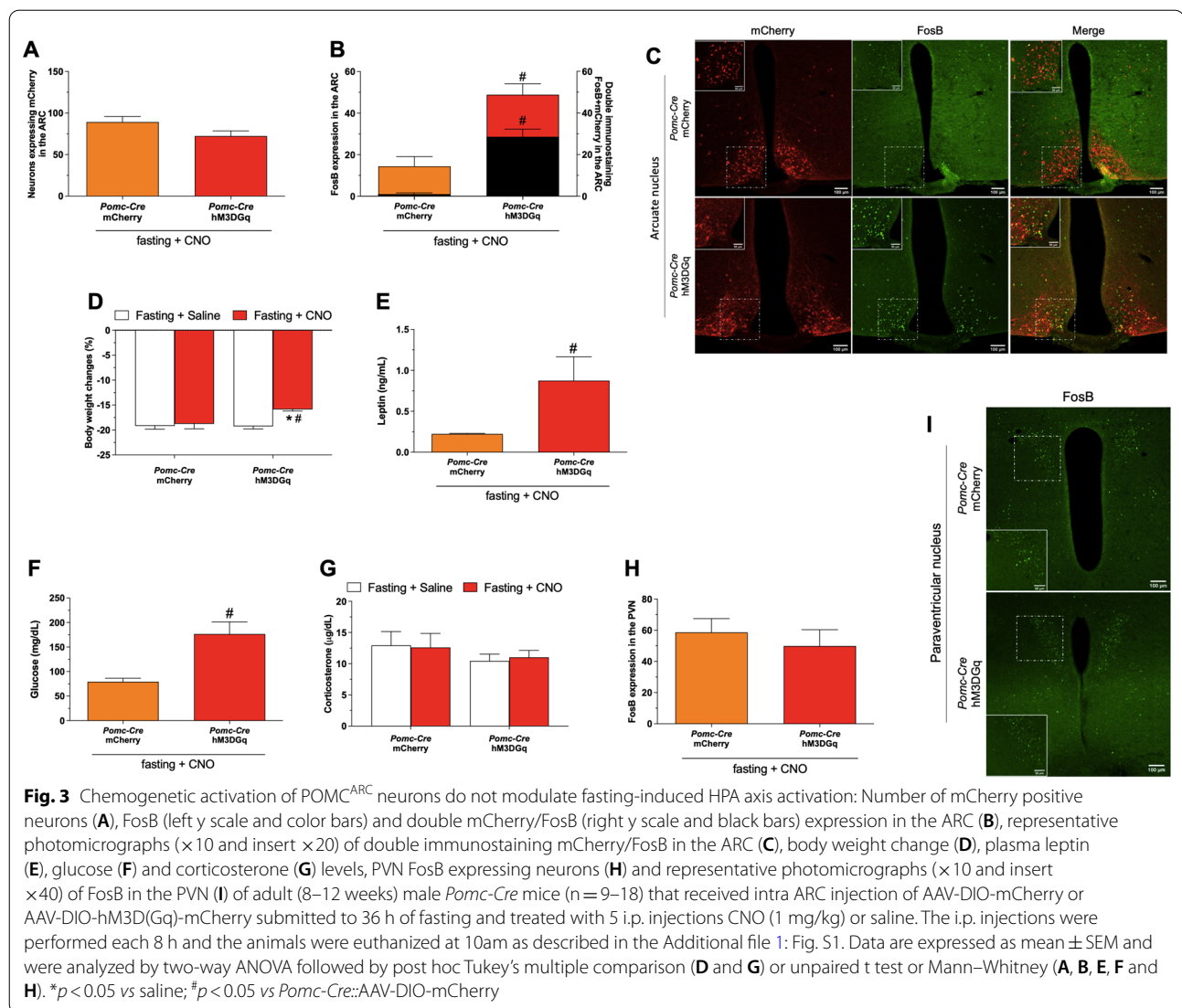
Fig. 2 Leptin treatment prevents HPA axis activation under fasting: Body weight change (A), plasma leptin (B) and glucose (C) levels, ARC gene expression (D), *Crf* gene expression in the PVN (E), plasma corticosterone levels (F), FosB (G) and double FosB/tdTomato (H) immunostaining in the PVN in 36 h-fasted adult (8–10 weeks) male mice ($n = 10-12$) treated with 4 injections (each 8 h) of saline, 0.5 $\mu\text{g/g}$ or 1 $\mu\text{g/g}$ of leptin (i.p.) and euthanized at 10 a.m. as also described in the Additional file 1: Fig. S1. Data from graphs A to F were obtained in WT animals, while graphs G and H and the photomicrographs ($\times 20$, insert $\times 10$) in I were obtained from *Crh-IRES-Cre:tdTomato* (red) mouse and submitted to immunostaining for FosB (green). Data are expressed as mean \pm SEM and were analyzed by one-way ANOVA followed by post hoc Tukey's multiple comparison or Kruskal–Wallis test followed by Dunn's multiple comparison. $*p < 0.05$ when comparing leptin 0.5 $\mu\text{g/g}$ or 1 $\mu\text{g/g}$ vs saline treatment in fasted mice

Surprisingly, activation of POMC_{ARC} reduced fasting-induced body weight loss (Fig. 3D, mCherry + saline = $-19.2 \pm 0.6\%$ BWC, mCherry + CNO = $-18.8 \pm 1.0\%$ BWC, hM3DGq + saline = $-19.3 \pm 0.6\%$ BWC and hM3DGq + CNO = $-15.8 \pm 0.3\%$ BWC, two-way ANOVA followed by post hoc Tukey's multiple comparison, * and # $p = 0.01$) and this response was associated with increased plasma leptin (Fig. 3E, mCherry = 0.2 ± 0.0 ng/mL and hM3DGq = 0.9 ± 0.3 ng/mL, Mann–Whitney test, $p = 0.01$) and glucose levels (Fig. 3F, mCherry = 79.3 ± 7.1 mg/dL and hM3DGq = 176.6 ± 24.8 mg/dL, Mann–Whitney test, $p = 0.001$). In addition, the specific activation of POMC_{ARC} had no effect on the increased plasma corticosterone levels in fasted animals (Fig. 3G, mCherry + saline = 12.9 ± 2.2 $\mu\text{g/dL}$, mCherry + CNO = 12.6 ± 2.2 $\mu\text{g/dL}$, hM3DGq + saline = 10.4 ± 1.1 $\mu\text{g/dL}$ and hM3DGq + CNO = 11.0 ± 1.1 $\mu\text{g/dL}$, two-way ANOVA followed by post hoc Tukey's multiple comparison). Fasting-induced FosB expression in PVN neurons was not affected by activation of POMC_{ARC} neurons

(Fig. 3H, I mCherry = 58.6 ± 8.9 FosB + cells and hM3DGq = 49.9 ± 10.4 FosB + cells, Mann–Whitney test, $p = 0.5$). Similar results to these described here were observed comparing Pomc-Cre and WT animals treated with AAV-DIO-hM3DGq-mCherry (Additional file 3: Fig.S3).

Chemogenetic inhibition of AgRP^{ARC} neurons reduces PVN neuronal activity without affecting plasma corticosterone levels in fasted animals

We observed similar mCherry expression after bilateral injections of AAV-DIO-hM4DGq and AAV-DIO-mCherry in *AgRP^{ARC}-Cre* animals (Fig. 4A, mCherry = 64.3 ± 3.9 mCherry + cells and hM4DGq = 54.3 ± 4.1 mCherry + cells, unpaired *t* test, $p = 0.1$). CNO treatment reduced FosB+mCherry colocalization (Fig. 4B, mCherry = 12.4 ± 2.4 FosB+mCherry cells and hM4DGq = 4.4 ± 0.4 FosB+mCherry cells, Mann–Whitney test, $p = 0.003$) in AgRP^{ARC} neurons in fasted animals expressing hM4DGq (Fig. 4B,C). The specific inhibition of AgRP^{ARC}



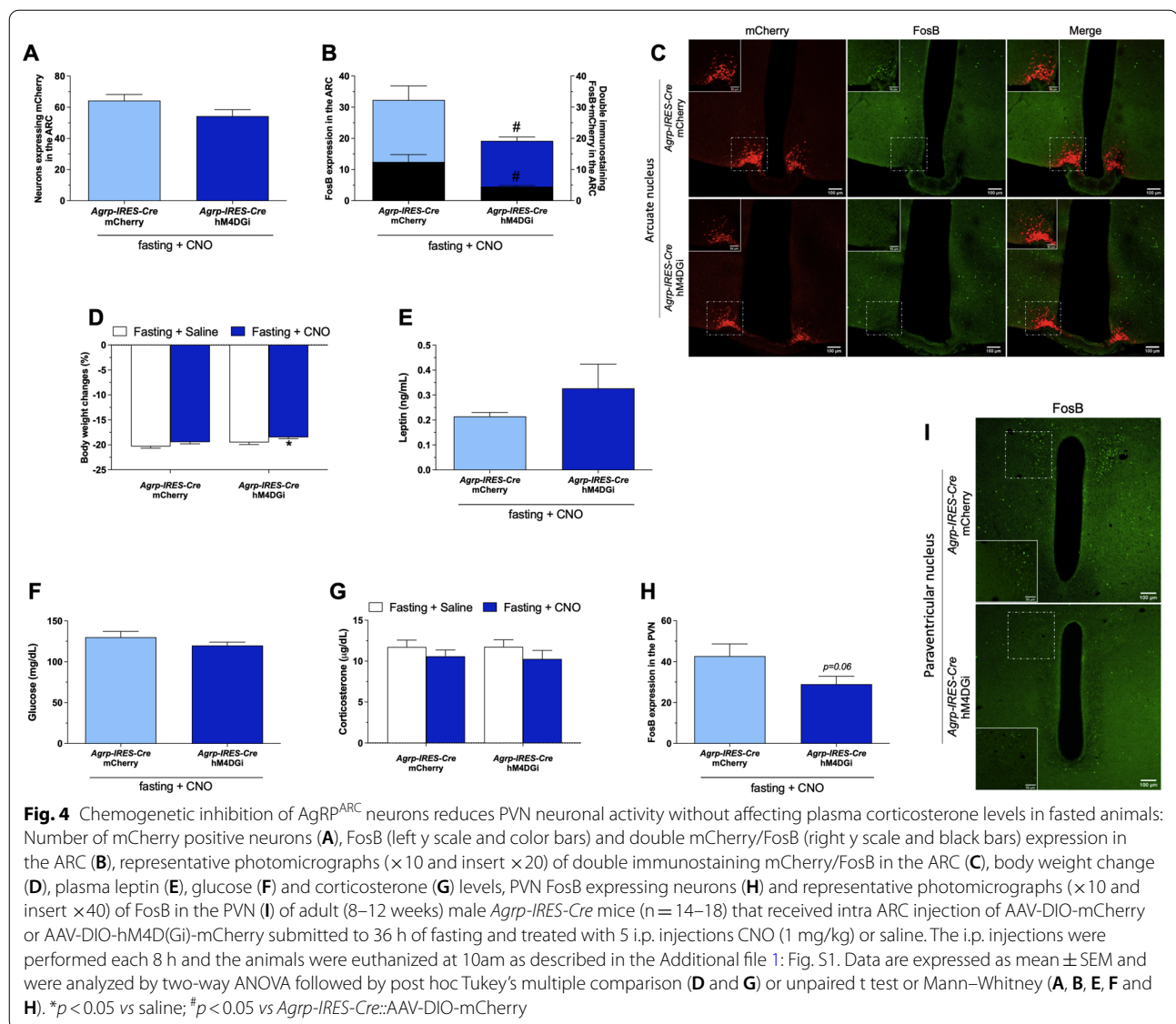
neurons reduced the activation of PVN neurons (Fig. 4H, I, mCherry=42.7±6.0 FosB+ cells and hM4DG= 29± 3.9 FosB+ cells, unpaired *t* test, *p*=0.0687) but had no effect on fasting-induced corticosterone secretion (Fig. 4G, mCherry+ saline = 11.7± 0.8 µg/dL, mCherry+ CNO= 10.6± 0.8 µg/dL, hM4DG+ saline = 11.7± 0.8 µg/dL and hM4DG+ CNO= 10.3± 1.0 µg/dL, two-way ANOVA followed by post hoc Tukey's multiple comparison).

We also observed reduced body weight loss (Fig. 4D, mCherry + saline = - 20.3 ± 0.3%BWC, mCherry + CNO = - 19.4 ± 0.3%BWC, hM4DG+ saline = - 19.5 ± 0.4%BWC and hM4DG+ CNO = - 18.5 ± 0.3%BWC, twoway ANOVA followed by post hoc Tukey's multiple comparison, **p* = 0.003) after activation of AgRP^{ARC} neurons and no difference in the reduction of plasma leptin (Fig. 4E, mCherry =

0.2 ± 0.0 ng/mL and hM4DG= 0.3 ± 0.1 ng/mL, Mann–Whitney test, *p* = 0.5) and glucose (Fig. 4F, mCherry = 130 ± 7.1 mg/dL and hM4DG= 119.8 ± 4.2 mg/dL, Mann–Whitney test, *p* = 0.3) levels between the groups. Similar results to these described here were obtained comparing *AgRP-IRES-Cre* and WT animals that received icv injection of AAV-DIO-hM4DG-mCherry (Additional file 4: Fig. S4).

Inhibition of AgRP^{ARC} neurons in fasted animals reduces CRF content in the PVN and increases its accumulation in the median eminence

In our CRF immunostaining study, we observed reduced CRF-IR in the PVN (Fig. 5B,D, mCherry=169.8±24 and hM4DG=96.8±14.5, unpaired *t* test, *p*=0.02), whereas the level of this peptide increased in the ME (Fig. 5C,E,



mCherry = 45.2 ± 14.5 CRF-IR and hM4DGi = 105.8 ± 14.3 CRF-IR, unpaired t test, $p = 0.001$) in *AgRP-IRES-Cre* animals expressing hM4DGi and treated with CNO. However, we observed no difference in the number of CRF+ cells (Fig. 5A,D, mCherry = 45.6 ± 12.4 and hM4DGi = 22.7 ± 6.2 , unpaired t test) in the PVN. We also observed similar results comparing *AgRP-IRES-Cre* and WT animals treated with AAV-DIO-hM4DGi-mCherry (Additional file 5: Fig. S5).

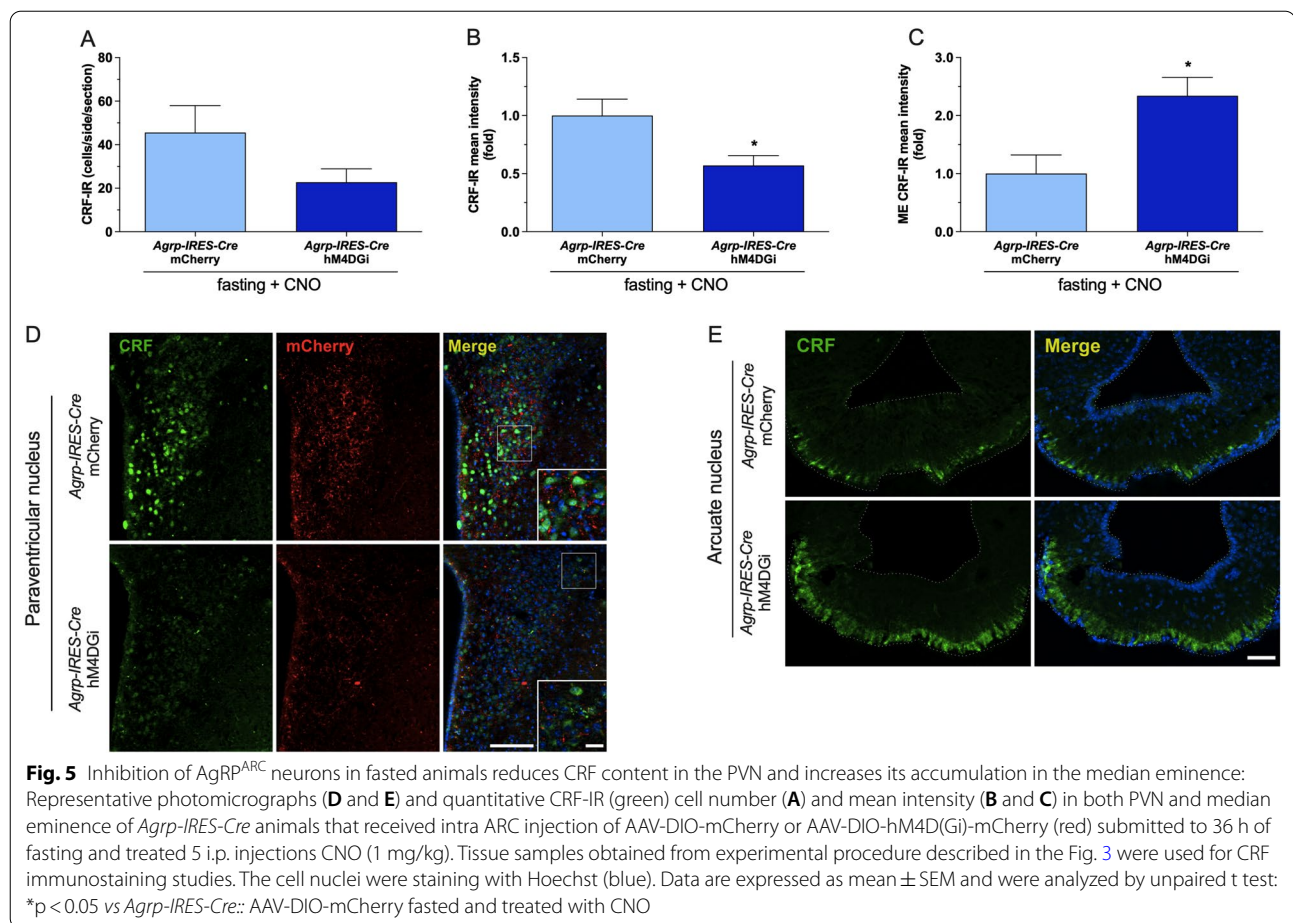
Discussion

In the present study we demonstrated the effects of food deprivation on the HPA axis activity and the involvement of $AgRP^{ARC}$ neurons in the gene expression/activation of CRF^{PVN} neurons, the major HPA axis controller.

It's well known that fasting activates HPA axis [9]. Here we demonstrated that the increased plasma

corticosterone levels observed in fasted mice was associated to increased mRNA expression and activity of CRF^{PVN} . The increased plasma glucocorticoid levels in fasted animals and humans are essential to the energy substrate utilization (fatty acids instead of carbohydrates) and to the activation of hepatic gluconeogenesis to avoid hypoglycemia [22, 23]. Interestingly, it has recently been demonstrated that hyperphagia caused by various energy-depleted states, such as food deprivation, hypoglycemia, or diabetes, is also dependent on increased plasma corticosterone levels and its actions on arcuate neurons controlling food consumption [24].

The reduction in body weight and the consequent decrease in plasma glucose and leptin levels in mice fasted for 36 h can contribute to the changes in the HPA axis activity [9–11]. Indeed, fasting-induced



hypoglycemia can recruit the counter-regulatory response and consequently increase glucagon, epinephrine and corticosterone secretion [25, 26]. Additionally, the decrease in the synthesis of leptin from the white adipose depots [27] leading to a reduction of plasma leptin levels is required for metabolic adaptations to reduce energy availability and activation of the counter-regulatory response [25].

Regarding the mRNA expression in the ARC, we observed increased mRNA expression of *Agrp*, *Npy* and *Gad65/67* in the ARC, and decreased *Pomc* mRNA expression in mice fasted for 36 h. These data reinforce the role and the responsiveness of neuropeptides/neurotransmitters expressed in ARC neurons in the control of energy homeostasis [7, 8, 10]. Together, our data indicate that a prolonged fasting period changes the mRNA expression and activity of CRF^{PVN} neurons in response to changes in ARC mRNA expression/activity of neuropeptides/neurotransmitters projecting to PVN.

Leptin can reduce or increase the HPA axis activity and its response it seems to be associated with the amount of energy available, i.e. in fasted animals the most prevalent

response observed in scientific studies is a decrease in plasma corticosterone levels after leptin administration [9, 11, 28]. Furthermore, even during food deprivation, this effect of leptin appears to be dependent on the level of the reduction of energy storage, as increased HPA activity was reported in studies using a prolonged period of fasting (e.g. 48 h) [9, 24] but not in 24 h fasted animals [24, 29]. In our study, we observed increased body weight loss and plasma corticosterone levels in animals fasted for 24 h, but higher body weight loss and plasma corticosterone levels after 36 h of fasting (Additional file 2: Fig. S2). The reduced mRNA expression of CRF^{PVN} and neuronal activity of CRF^{PVN} neurons are in accordance with the inhibitory role of leptin on the HPA axis activity [9, 28].

The effects of leptin on the CRF gene expression and CRF^{PVN} neuronal activity can not be mediated by direct leptin signaling, since LepR is not expressed in CRF^{PVN} neurons [13]. Additionally, ARC neurons have their gene expression (Fig. 2D) and activity modulated by leptin [12, 14] and, as we previously cited, icv or even site-specific

administration of the neuropeptides/neurotransmitters produced by ARC modulates the HPA axis activity [30, 31]. Therefore, the changes in the ARC mRNA could account for the reduction in the HPA axis activity after leptin administration. In addition, the decrease of plasma corticosterone levels in fasted mice under leptin treatment can contribute to the reduction of plasma glucose levels. However, leptin may also affect other key glucoregulatory mechanisms (i.e., sympathetic nervous system activity) [22, 32–34] to modulate plasma glucose levels. Together, our data reinforce the inhibitory role of leptin in the control of CRF^{PVN}. Furthermore, a direct leptin signaling on adrenal gland [35] and/or indirect actions via ARC neurons could also be involved in the reduction of plasma corticosterone levels after leptin treatment to fasted animals.

POMC^{ARC} neurons project to the PVN [17] and are modulated by fasting [36] and leptin [14]. Thus, we investigated the consequences of the chemogenetic activation of POMC^{ARC} on plasma corticosterone levels in 36 h-fasted mice. Despite the effective chemogenetic activation of POMC^{ARC} neurons in fasted animals expressing the excitatory DREADD, we observed no effect on PVN neuronal activity and on the increased plasma corticosterone levels induced by food deprivation. POMC^{ARC} neurons are heterogenous regarding their responsiveness to hormones such as leptin [37] and particularly regarding to the type of the neurotransmitter they express (e.g., AgRP, NPY and GABA) [38, 39]. Therefore, the heterogeneity of these neurons must be considered before definitely excluding their participation in the control of the HPA axis activity in fasting conditions. A study using the same lineage of animals reported that POMC neurons project to the adrenal gland, and the deletion of *LepR* in this neuronal population does not modify the activation of SNS induced by icv leptin [40]. We cannot exclude the possibility that the development of compensatory mechanism during development could have affected the evaluation of the role of POMC^{ARC} neurons in the effects of leptin on ANS in the Bell and cols study [40]. Thus, our data demonstrated that the prolonged activation of the heterogenous population of POMC^{ARC} neurons do not modify the corticosterone plasma levels during fasting.

Additionally, activation of POMC^{ARC} reduced fasting-induced body weight loss and increased plasma leptin and glucose levels. Notably, only one-third of CNO-treated *Pomc-Cre::hM3DGq* mice had plasma leptin levels higher than the control group suggesting that the effect of prolonged activation of POMC^{ARC} neurons on plasma leptin levels was secondary to body weight loss instead of a direct effect of POMC^{ARC} neuronal modulation, as described by others [41]. Our data about body weight change and plasma glucose levels in fasted

animals subjected to prolonged POMC^{ARC} activation are contradictory to the classical role of these neurons on energy and glucose homeostasis. Despite some studies have observed the expected effect on energy balance after chemogenetic modulation of POMC^{ARC} neurons (i.e. reduced food intake after activation) [42, 43], there are divergent results about its effect on glucose homeostasis. So, it was reported that the selective activation of POMC^{ARC} neurons can reduce pyruvate-induced hyperglycemia [44], while other study described no effect on plasma glucose levels after POMC^{ARC} modulation [45] or even a fall in glycemia after inhibition of POMC^{ARC} neurons [42]. Therefore, our data support the heterogeneity of these neurons and suggests that the responses observed in our study are involved with the activation of a subset of POMC^{ARC} neuron that could also produce AgRP, NPY and/or GABA that could inhibit energy metabolism.

Given that the food consumption-effects induced by activation of AgRP^{ARC} neurons are mediated, at least in part, by modulating the activity of PVN neurons [46–48] and that these ARC neurons are inhibited by leptin [10] we also investigated whether the specific inhibition of AgRP^{ARC} neuronal activity could modulate plasma corticosterone levels in fasted animals. Our findings show that inhibiting AgRP^{ARC} neurons has no effect on fasting-increased plasma corticosterone levels, but it is effective in reducing PVN neuron activity. The lack of changes in corticosterone secretion after inhibiting of AgRP^{ARC} neuronal activity is opposite to the results reported by pharmacological studies, which observed increased corticosterone secretion after intra PVN administration of NPY [15, 16], the neuropeptide coexpressed with AgRP^{ARC}. On the other hand, the present data on FosB study indicates that specific inhibition of AgRP^{ARC} neurons reduces the activity of PVN neurons. Therefore, according to an excitatory role of NPY on PVN neurons, it was described that the NPYr2 can be coupled to Gq signaling [49]. Therefore, inhibition of AgRP^{ARC} neurons could reduce NPY signaling via NPYr2 expressed in the PVN that in turn could lead to a decreased PVN neuronal activity in fasted conditions. However, we cannot exclude an indirect effect of AgRP^{ARC} neurons on the PVN activity, since AgRP^{ARC} neurons project to other brain sites that in turn are directly connected to PVN neurons [17, 18].

Recently, it was demonstrated that GABAergic neurons from ARC are directly connected to CRF^{PVN} neurons, supporting the involvement of this ARC neurotransmitter in the control of the HPA axis [18]. Interestingly, under prolonged hyperosmotic stress, GABAergic signaling in the PVN is switched from inhibitory to excitatory [50, 51]. Moreover, administration of GABA_AR agonist

can induce CRF releasing in the median eminence [52]. Therefore, the inhibition of NPY and GABA release from AgRP^{ARC} neurons could also contribute to the reduced neuronal activity in the PVN during fasting.

As expected inhibition of AgRP^{ARC} reduced fasting-induced body weight loss, but didn't change the effects of fasting on plasma leptin and glucose levels. AgRP^{ARC} neurons are known to negatively modulate the metabolism and part of these responses can be associated with a change in the thyroid axis activity and energy expenditure [53]. Therefore, reduction in energy expenditure after inhibition of AgRP^{ARC} can be associated with the reduced body weight loss.

Since we had observed reduced PVN neuronal activity after inhibition of AgRP^{ARC} neurons in fasted animals, we also investigated the content of CRF in the PVN and its releasing in the median eminence in these animals. Interestingly, our data indicates AgRP^{ARC} neurons can modulate the synthesis and secretion of CRF^{PVN} during metabolic stress. Our results corroborate the data from Kakizawa and Cols that observed increased CRF release in the ME after administration of GABA_AR agonist [52]. Therefore, our findings are consistent with other studies indicating an excitatory role of AgRP^{ARC} neurons on CRF^{PVN} expression/activity [15, 51, 52, 54] and highlight AgRP^{ARC} neurons as a component of the neurocircuitry controlling the activity of CRF^{PVN} neurons during fasting.

Despite the reduced CRF content in the medial parvocellular PVN subdivision and its accumulation in the ME, plasma corticosterone levels were not reduced in *Agrp-IRES-Cre* mice expressing hM4DGi treated with CNO. To conciliate these results, we need to consider the involvement of different pathways and mechanisms that underlie stress-induced increase in plasma corticosterone levels. So, considering that AgRP^{ARC} neuronal inhibition induced a slight fall in PVN FosB expression, other PVN peptides involved in the control of pituitary-ACTH activity and ANS, such as vasopressin and even CRF expressed in PVN autonomic neurons, could act to maintain the increased plasma corticosterone levels via modulation of adrenal gland activity (neural mechanisms or dependent of ACTH) [55–58]. Additionally, mechanisms associated with changes in the sensitivity to the ACTH [59] and/or peripheral glucocorticoid metabolism [60, 61] may contribute to the preserved corticosterone secretion in *Agrp-IRES-Cre::hM4DGi* mice treated with CNO. Therefore, the existence of redundant pathways/neurocircuitries and mechanisms involved in the control of HPA axis are probably underlying the maintenance of increased plasma corticosterone levels in fasted animals after the selective inhibition of AgRP^{ARC} neurons.

Finally, since CRF^{PVN} neurons are involved in the control of endocrine, autonomic, and behavioral responses

to stress [2–4], we speculate that its reduced content in the PVN with the inhibition of AgRP^{ARC} neurons could be related to the modulation of other stress-related responses that were not investigated in our study. Given that AgRP^{ARC} neurons modulate several motivational components of food consumption [54] and that CRF^{PVN} also controls several behavioral stress-related responses [4], part of those behavioral changes elicited by AgRP^{ARC} neurons could be associated to change in the activity of CRF^{PVN} neurons.

Conclusion

Our study reinforces the recruitment of HPA axis during fasting and the involvement of leptin in this response. Additionally, we demonstrate that AgRP^{ARC}, but not POMC^{ARC}, are part of the neurocircuitry involved in the control of CRF^{PVN} neurons activity during fasting. The uncovering of the mechanism and neurocircuitry involved in the coupling of HPA axis activity to changes in peripheral energy stores could be considered an important strategy to the development of new therapies to treat of pathologies associated with the disturbance of the HPA axis, including obesity and metabolic syndrome.

Methods

Animals

All procedures were approved by the Ethical Committee for Animal Use of the University of Ribeirao Preto (12/2017, February 2018) and Federal University of Sao Paulo (07/2020-1276210720). C57BL6 male mice were obtained from Central Animal Facility of the University of Sao Paulo-Campus Ribeirao Preto. Male *Agrp-IRES-Cre*, *Pomc-Cre* mice, *Crh-IRES-Cre* and the Cre-inducible tdTomato-reporter mouse were purchased from JAX mice (Bar Harbor, ME) and genotyped as previously described [62, 63]. The animals were housed in groups under controlled light (12:12 h light–dark cycle; lights off at 06:00 p.m.) and temperature conditions (23 ± 2 °C), with free access to water and food, unless otherwise stated.

Experimental procedures

For all protocols, mice were single housed for at least 1 week before the beginning of the experiments and habituated to researcher manipulation. Flow charts of the experimental procedures are described in Additional file 1: Fig. S1.

For the fasting study, mice were weighed and maintained on regular diet or fasted for 36 h. At the end of the experiment (10 a.m.) they were weighed again and immediately decapitated for blood (heparinized tube) and tissue collection. In the leptin treatment experiment, fasted mice were treated with 4 i.p. injections of saline or

leptin [Millipore (Burlington, MA)—doses of 0.5 µg/g or 1 µg/g] at 6am, 2 pm, 10 p.m. of day 2 and at 6am on day 3 (last day). At 10 a.m. fasted mice treated with saline or leptin were weighed again and decapitated for blood and tissue collection. Perfusion for immunostaining studies (described below) were performed using *Crh-IRES-Cre:tdTomato*-reporter mouse.

For DREADDs experiments, 2 weeks after surgery, WT, *Pomc-Cre* or *Agrp-IRES-Cre* mice were fasted and treated with 5 i.p. injections of saline + 1% DMSO (10 p.m.–day1, 6 a.m., 2 p.m., 10 p.m.–day2 and 6 a.m.–day3) and their blood collected via submandibular bleed. After 2 weeks the same mice were fasted again and treated with 5 i.p. injections of Clozapine-N-Oxide [Cayman Chemical (Ann Arbor, MI)—1 mg/kg] (10 p.m.–day1, 6 a.m., 2 p.m., 10 p.m.–day2 and 6 a.m.–day3) and then quickly anesthetized with isoflurane and perfused for blood and brain collection.

Viral vectors microinjection and stereotaxic surgery

Anesthetized mice were submitted to stereotaxic surgery for Adeno-associated viral (AAV) injection [64]. A volume of 200 nL of pAAV8-hSyn-DIO-hM3D(Gq)-mCherry, pAAV8-hSyn-DIO-hM4D(Gi)-mCherry or pAAV8-hSyn-mCherry (Addgene, Watertown, MA) was bilaterally injected into the ARC (AP: − 1.4, DV: − 5.85 and ML: ± 0.3 from bregma) during 5 min (40 nL/min); the pipette was removed 5 min after injection. The AAVs contain either the excitatory or inhibitory DREADD and the mCherry sequence in reverse orientation and, flanked by loxP sites. The presence of Cre-recombinase flips the DNA so that it can be transcriptionally expressed. We used mice that express Cre-recombinase in either AgRP/ NPY neurons (*Agrp-IRES-Cre* mice) or POMC neurons (*Pomc-cre* mice). We also want to mention that a subset of POMC neurons colocalize with NPY/AgRP during embryonic development [38, 39].

After the surgery, mice had 2 weeks to recover from the surgical procedure and to acclimate to be individually housed before the beginning of the experiments. The 2 weeks period was also necessary for the expression of the DREADDs. To confirm the correct injection and expression of the DREADDs, mCherry expression was visualized in the ARC.

Transcardiac perfusion, tissue collection and immunostaining

Mice were perfused and the tissue processed to obtain 25-µm coronal sections as previously described [40, 42, 46]. Briefly, to perform FosB immunostaining, brain sections were rinsed with Phosphate Buffered Saline (PBS; 1×, pH 7.4), pre-treated for 1 h in PBS containing 5% normal donkey serum (Jackson ImmunoResearch

Laboratories, Inc., West Grove, PA, USA) and 0.3% Triton X-100 and then incubated with a rabbit anti-FosB polyclonal IgG (1:1000, Santa Cruz Biotechnology, #sc48) overnight at room temperature. After rinsing, sections were incubated with a donkey anti-rabbit IgG conjugated with Alexa 488 secondary antibody (1:400; Jackson ImmunoResearch Laboratories, Inc., West Grove, PA, USA). The mCherry fluorescence could be observed without immunostaining. Finally, the sections were coverslipped with Fluoromont-G mounting medium (Sigma-Aldrich, USA).

We performed CRF immunofluorescence studies as described before [65]. Briefly, sections were pre-treated with blocking solution (2% normal horse serum and 0.25% Triton-X) and then incubated with a rabbit anti-CRH antibody (1:1000) for 48 h at 4 °C. This antibody recognizes mature CRF (1–41) and full pre-proCRF prohormone [66]. Next, sections were incubated with a goat anti-rabbit Alexa Fluor 488 antibody (1:1000, Thermo Fisher, Waltham, MA) for 2 h. Brain sections were sequentially mounted on glass slides and coverslipped with mounting media.

Quantitative neuroanatomical analysis

A Zeiss inverted Fluorescence motorized phase contrast microscope was used to acquire the photomicrographs associated to FosB data. Two or three images from each animal were quantified for mCherry, FosB only or double FosB + mCherry using Image J software (NIH, Bethesda, MD). Only animals mCherry+ in both sides of the ARC were used in the experiments. We used mCherry as marker of specificity and efficiency of viral vector transduction and FosB as a marker of prolonged neuronal activity. FosB immunofluorescence + tdTomato (reporter animals) were used to indicate changes in CRF^{PVN} neuronal activity.

For CRF-IR studies, fluorescence images were acquired with 20×/0.80 and 40×/0.95 objectives using a Zeiss AxioObserver D1 equipped with an Apotome.2 structured illumination module and an AxioCam 506 monochrome camera. All image processing and analysis were performed in the ImageJ-based open-source image-processing package Fiji (NIH, Bethesda, MD) [67]. Fluorescent signal corresponding to CRH+ was blindly and bilaterally quantified in the PVN and EM. The average fluorescence intensity was quantified in low magnification (20×) images of one complete series of coronal sections per brain between bregma − 0.58 and − 0.94 mm for the PVN and between bregma − 1.58 and − 1.94 mm for the EM [68]. For each image, the histogram of signal intensity was obtained, and the tissue background level was estimated by fitting a Gaussian curve, which coincided with the dominant peak. With these parameters,

a specific signal detection threshold was calculated, which was defined as the mean of the distribution plus five standard deviations. A region of interest was created according to this threshold. The mean fluorescence intensity was quantified in each image within this thresholded region.

Brain microdissection, RNA isolation and qPCR

The PVN and ARC microdissections were performed with a stainless-steel punch needle (1.0 mm diameter) in a cryostat according to the coordinates from -0.18 to -1.055 mm (~ 800 μ m) and from -1.055 to -2.255 mm (1200 μ m) bregma, respectively [68].

Total RNA from PVN and ARC were extracted using RNeasy Mini Kit (QIAGEN, Hilden, Germany) and reverse transcribed (QuantiTect RT Kit, QIAGEN). For TaqMan gene expression assay, qPCR master mix QuantiNova kit (QIAGEN) and specific primers from Integrated DNA Technology (IDT, Coralville, IA) were used. Quantitative PCR was performed in triplicate using the QuantStudio 5 (Applied Biosystems). Relative mRNA levels were calculated using the standard curve method and normalized to the level of b-actin.

Plasma hormones and glucose determinations

Plasma corticosterone levels were determined by specific radioimmunoassays after extraction with ethanol, as previously described [69]. Plasma leptin (Millipore, Burlington, MA) and glucose (Doles Reagents, Goiania, Brazil) concentrations were measured using commercial kits.

Statistical analysis

The data are expressed as mean \pm SEM. Samples were tested for regular distribution using Shapiro–Wilk normality test (Prism9.0-GraphPad software, San Diego, CA). We used one- or two-way ANOVA, followed by the appropriate post hoc tests, or an unpaired Student's t test (or the Mann–Whitney test for non-parameteric data). Differences were accepted as significant if $p < 0.05$. The specific statistical tests that were used are indicated in the figure legends.

Supplementary Information

The online version contains supplementary material available at <https://doi.org/10.1186/s13578-022-00853-z>.

Additional file 1: Figure S1. Experimental designs used in the protocols performed to obtain data showed in Fig. 1 (fasting and fasting + leptin studies) and Figs. 2, 3 and 4.

Additional file 2: Figure S2. Prolonged fasting increases *Crf* mRNA expression in the PVN and induces higher corticosterone secretion: Experimental design (A), body weight change (B), plasma leptin (C), glucose (D) and corticosterone (E) levels, changes in the mRNA expression in the

PVN (F) and ARC (G) of adult (8–10 weeks) WT mice fed or fasted for 24 h or 36 h ($n = 8–10$). Data are expressed as mean \pm SEM and were analyzed by one-way ANOVA and Tukey test for multiple comparisons were used for samples that passed in the normality test (B, C, D and E) otherwise Kruskal–Wallis test followed by Dunn's multiple comparisons were used (F and G); * $p < 0.05$ vs fed and # $p < 0.05$ vs 24 h fasting.

Additional file 3: Figure S3. Chemogenetic activation of POMC^{ARC} neurons do not modulate fasting-induced HPA axis activation: FosB expression in the ARC (A), representative photomicrographs (10 \times and insert 20 \times) of double immunostaining mCherry/FosB in the ARC (C), body weight change (D), plasma leptin (E), glucose (F) and corticosterone (G) levels, PVN FosB expressing neurons (H) and representative photomicrographs (10 \times and insert 40 \times) of FosB in the PVN (I) of adult (8–12 weeks) male WT or *Pomc-Cre* mice ($n = 8–18$) that received intra ARC injection AAV-DIO-hM3D(Gq)-mCherry submitted to 36 h of fasting and treated with 5 i.p. injections CNO (1 mg/kg) or saline. The i.p. injections were performed each 8 h and the animals were euthanized at 10am as described in the Additional file 1: Fig. S1. Data are expressed as mean \pm SEM and were analyzed by two-way ANOVA followed by post hoc Tukey's multiple comparison (C and F) or unpaired t test. * $p < 0.05$ vs saline; # $p < 0.05$ vs *Pomc-Cre::AAV-DIO-mCherry*.

Additional file 4: Figure S4. Chemogenetic inhibition of AgRP^{ARC} neurons reduces PVN neuronal activity without affecting plasma corticosterone levels in fasted animals: FosB expression in the ARC (A), representative photomicrographs (10 \times and insert 20 \times) of double immunostaining mCherry/FosB in the ARC (C), body weight change (D), plasma leptin (E), glucose (F) and corticosterone (G) levels, PVN FosB expressing neurons (H) and representative photomicrographs (10 \times and insert 40 \times) of FosB in the PVN (I) of adult (8–12 weeks) male WT or *AgRP-IRES-Cre* mice ($n = 8–18$) that received intra ARC injection AAV-DIO-hM4D(Gi)-mCherry submitted to 36 h of fasting and treated with 5 i.p. injections CNO (1 mg/kg) or saline. The i.p. injections were performed each 8 h and the animals were euthanized at 10am as described in the Additional file 1: Fig. S1. Data are expressed as mean \pm SEM and were analyzed by two-way ANOVA followed by post hoc Tukey's multiple comparison (C and F) or unpaired t test. * $p < 0.05$ vs saline; # $p < 0.05$ vs *AgRP-IRES-Cre::AAV-DIO-mCherry*.

Additional file 5: Figure S5. Inhibition of AgRP^{ARC} neurons reduces PVN CRF content and induces its accumulation in the median eminence of fasted mice: representative photomicrographs (D and E) and quantitative CRF-IR (green) cell number (A) and mean intensity (B and C) in both PVN and median eminence of WT or *AgRP-IRES-Cre* animals that received intra ARC injection of AAV-DIO-hM4D(Gi)-mCherry (red) submitted to 36 h of fasting and treated 5 i.p. injections CNO (1 mg/kg). Tissue samples obtained from experimental procedure described in the Fig. 3 were used for CRF immunostaining studies. The cell nuclei were staining with Hoechst (blue). Data are expressed as mean \pm SEM and were analyzed Unpaired t test: # $p < 0.05$ vs WT::AAV-DIO-hM4D(Gi)-mCherry fasted and treated with CNO.

Acknowledgements

We would like to thank Maria Valci dos Santos, Milene Mantovani and Gabriel Esquitini for their excellent technical assistance. We also want to thank to Dr. Lucila Elias for the kindly donation of *AgRP-IRES-Cre* and *Pomc-Cre* and Dr. Jose Donato Jr. for the donation of tdTomato-reporter mouse. Finally, we are grateful to Dr. Ronaldo de Carvalho Araujo, Dr. Alexandre Budu and Dr. Gerson Dierley Keppeke for the support in the image acquisition.

Author contributions

RR conceptualized the study, acquired funding, prepared figures and wrote the original draft. RR and KV designed the experiments. ACAF and RR performed the experiments with animals and analyzed the data. LGV, TN and CGR performed experiments related to DREADDs. FPO performed mCherry + FosB and tdTomato + FosB studies. MP and FG performed and analyzed CRF IF experiments. ACAF, FPO, FG, LGV, JDJ, KV, JAR, AM, GF, MP and LLKE read and provided feedback on manuscript and figures. All authors read and approved the final manuscript.

Funding

This work was supported by São Paulo Research Foundation (FAPESP—Grant RR: 2016/17968-6; Grant ASM: 2019/27581-0), Brazilian Federal Agency for Support and Evaluation of Graduate Education (CAPES: FPO—88887.474642-2020-00), National Council for Scientific and Technological Development (CNPq—ASM:309882/2020-6), Fondo para la Investigación Científica y Tecnológica (PICT2016-1084, PICT2017-3196, PICT2019-3054) and CONICET (PUE-2017).

Availability of data and materials

All the data related to this manuscript are available with the corresponding author.

Declarations

Ethics approval and consent to participate

All the experimental procedures were conducted in accordance with the animal protection laws in Brazil and approved by the Ethical Committee for Animal Use of the University of Ribeirão Preto (12/2017, February 2018) and Federal University of Sao Paulo (07/2020-1276210720).

Consent for publication

Not applicable.

Competing interests

The authors declare that they have no competing interests.

Author details

¹Department of Biotechnology, University of Ribeirão Preto, Ribeirão Preto, SP 14096-900, Brazil. ²Department of Physiology, Ribeirão Preto Medical School, University of Sao Paulo, Ribeirão Preto, SP 14049-900, Brazil. ³Department of Physiology and Biophysics, Institute of Biomedical Sciences, University of Sao Paulo, São Paulo, SP 05508-000, Brazil. ⁴Department of Endocrinology, Diabetes and Metabolism and the Weill Center for Metabolic Health, Weill Cornell Medical College, New York, NY 10021, USA. ⁵Laboratory of Neurophysiology of the Multidisciplinary Institute of Cell Biology (IMBICE, Argentine Research Council (CONICET) and Scientific Research Commission, Province of Buenos Aires (CIC-PBA), National University of La Plata, La Plata, 403, Buenos Aires, Argentina. ⁶Department of Biophysics, Paulista Medical School, Federal University of Sao Paulo, São Paulo, SP CEP 04023-062, Brazil.

Received: 12 April 2022 Accepted: 14 July 2022

Published online: 28 July 2022

References

- Miller WL. The hypothalamic-pituitary-adrenal axis: a brief history. *Horm Res Paediatr*. 2018;89(4):212–23. <https://doi.org/10.1159/000487755>.
- Carlin KM, Vale WW, Bale TL. Vital functions of corticotropin-releasing factor (CRF) pathways in maintenance and regulation of energy homeostasis. *Proc Acad Sci USA*. 2006;103(9):3462–7. <https://doi.org/10.1073/pnas.0511320103>.
- Chrousos GP. Stress and disorders of the stress system. *Nat Rev Endocrinol*. 2009;5(7):374–81. <https://doi.org/10.1038/nrendo.2009.106>.
- Füzesi T, Daviu N, Wamsteeker Cusulin JI, Bonin RP, Bains JS. Hypothalamic CRH neurons orchestrate complex behaviours after stress. *Nat Commun*. 2016;7:11937. <https://doi.org/10.1038/ncomms11937>.
- Björntorp P, Rosmond R. The metabolic syndrome—a neuroendocrine disorder? *Br J Nutr*. 2000. <https://doi.org/10.1017/s0007114500000957>.
- Anagnostis P, Athyros VG, Tziomalos K, Karagiannis A, Mikhailidis DP. The pathogenetic role of cortisol in the metabolic syndrome: a hypothesis. *J Clin Endocrinol Metab*. 2009. <https://doi.org/10.1210/jc.2009-0370>.
- Coppari R, Björbaek C. Leptin revisited: its mechanism of action and potential for treating diabetes. *Nat Rev Drug Discov*. 2012. <https://doi.org/10.1038/nrd3757>.
- Rosen ED, Spiegelman BM. Adipocytes as regulators of energy balance and glucose homeostasis. *Nature*. 2006. <https://doi.org/10.1038/nature05483>.
- Ahima RS, Prabakaran D, Mantzoros C, Qu D, Lowell BB, Maratos-Flier E, et al. Role of leptin in the neuroendocrine response to fasting. *Nature*. 1996;382(6588):250–2. <https://doi.org/10.1038/382250a0>.
- Morton GJ, Meek TH, Schwartz MW. Neurobiology of food intake in health and disease. *Nat Rev Neurosci*. 2014;15(6):367–78. <https://doi.org/10.1038/nrn3745>.
- Perry RJ, Zhang XM, Zhang D, Zhang D, Kumashiro N, Camporez JPG, et al. Leptin reverses diabetes by suppression of the hypothalamic-pituitary-adrenal axis. *Nat Med*. 2014;20(7):759–63. <https://doi.org/10.1038/nm.3579>.
- Hwa JJ, Fawzi AB, Graziano MP, Ghibaudi L, Williams P, Van Heek M, et al. Leptin increases energy expenditure and selectively promotes fat metabolism in ob/ob mice. *Am J Physiol Regul Integr Comp Physiol*. 1997. <https://doi.org/10.1152/ajpregu.1997.272.4.R1204>.
- Scott MM, Lachey JL, Sternson SM, Lee CE, Elias CF, Friedman JM, et al. Leptin targets in the mouse brain. *J Compar Neurol*. 2009;514(5):518–32. <https://doi.org/10.1002/cne.22025>.
- Baver SB, Hope K, Guyot S, Björbaek C, Kaczorowski C, O'Connell KMS. Leptin modulates the intrinsic excitability of AgRP/NPY neurons in the arcuate nucleus of the hypothalamus. *J Neurosci*. 2014;34(16):5486–96. <https://doi.org/10.1523/JNEUROSCI.4861-12.2014>.
- Inoue T, Inui A, Okita M, Sakatani N, Oya M, Morioka H, et al. Effect of neuropeptide Y on the hypothalamic-pituitary-adrenal axis in the dog. *Life Sci*. 1989;44(15):1043–51. [https://doi.org/10.1016/0024-3205\(89\)90556-0](https://doi.org/10.1016/0024-3205(89)90556-0).
- Albers HE, Ottenweller JE, Liou SY, Lumpkin MD, Anderson ER. Neuropeptide Y in the hypothalamus: effect on corticosterone and single-unit activity. *Am J Physiol Regul Integr Comp Physiol*. 1990. <https://doi.org/10.1152/ajpregu.1990.258.2.R376>.
- Wang D, He X, Zhao Z, Feng Q, Lin R, Sun Y, et al. Whole-brain mapping of the direct inputs and axonal projections of POMC and AgRP neurons. *Front Neuroanat*. 2015;9:40. <https://doi.org/10.3389/fnana.2015.00040>.
- Yuan Y, Wu W, Chen M, Cai F, Fan C, Shen W, et al. Reward inhibits paraventricular CRH neurons to relieve stress. *Curr Biol*. 2019;29(7):1243–1251.e4. <https://doi.org/10.1016/j.cub.2019.02.048>.
- Tillakaratne NJ, Medina-Kauwe L, Gibson KM. Gamma-Aminobutyric acid (GABA) metabolism in mammalian neural and nonneural tissues. *Compar Biochem Physiol Part A Physiol*. 1995;112(2):247–63. [https://doi.org/10.1016/0306-9629\(95\)00099-2](https://doi.org/10.1016/0306-9629(95)00099-2).
- Heilig M. The NPY system in stress, anxiety and depression. *Neuropeptides*. 2004;38(4):213–24. <https://doi.org/10.1016/j.nepep.2004.05.002>.
- Cone RD. Anatomy and regulation of the central melanocortin system. *Nat Neurosci*. 2005;8(5):571–8. <https://doi.org/10.1038/nn1455>.
- Schwartz MW, Seeley RJ. Neuroendocrine responses to starvation and weight loss. *N Engl J Med*. 1997;336(25):1802–11. <https://doi.org/10.1056/NEJM199706193362507>.
- Zhang S, Lv F, Yuan Y, Fan C, Li J, Sun W, et al. Whole-brain mapping of monosynaptic afferent inputs to cortical CRH neurons. *Front Neurosci*. 2019. <https://doi.org/10.3389/fnins.2019.00565>.
- Perry RJ, Resch JM, Douglass AM, Madara JC, Rabin-Court A, Kucukdereli H, Wu C, Song JD, Lowell BB, Shulman GI. Leptin's hunger-suppressing effects are mediated by the hypothalamic-pituitary-adrenocortical axis in rodents. *Proc Natl Acad Sci USA*. 2019;116(27):13670–9. <https://doi.org/10.1073/pnas.1901795116> (Epub 2019 Jun 18).
- Flak JN, Patterson CM, Garfield AS, D'Agostino G, Goforth PB, Sutton AK, et al. Leptin-inhibited PBN neurons enhance responses to hypoglycemia in negative energy balance. *Nat Neurosci*. 2014;17(12):1744–50. <https://doi.org/10.1038/nn.3861>.
- Garfield AS, Shah BP, Madara JC, Burke LK, Patterson CM, Flak J, et al. A parabrachial-hypothalamic cholecystokinin neurocircuit controls counterregulatory responses to hypoglycemia. *Cell Metab*. 2014;20(6):1030–7. <https://doi.org/10.1016/j.cmet.2014.11.006>.
- Trayhurn P, Thomas ME, Duncan JS, Rayner DV. Effects of fasting and refeeding on ob gene expression in white adipose tissue of lean and obese (ob/ob) mice. *FEBS Lett*. 1995;368(3):488–90. [https://doi.org/10.1016/0014-5793\(95\)00719-p](https://doi.org/10.1016/0014-5793(95)00719-p).
- Roubos EW, Dahmen M, Kozicz T, Xu L. Leptin and the hypothalamo-pituitary-adrenal stress axis. *Gen Comp Endocrinol*. 2012. <https://doi.org/10.1016/j.ygcen.2012.01.009>.
- Huang Q, Rivest R, Richard D. Effects of leptin on corticotropin-releasing factor (CRF) synthesis and CRF neuron activation in the paraventricular

- hypothalamic nucleus of obese (ob/ob) mice. *Endocrinology*. 1998;139(4):1524–32. <https://doi.org/10.1210/endo.139.4.5889>.
30. Xiao E, Xia-Zhang L, Vulliamoz NR, Ferin M, Wardlaw SL. Agouti-related protein stimulates the hypothalamic-pituitary-adrenal (HPA) axis and enhances the HPA response to interleukin-1 in the primate. *Endocrinology*. 2003;144(5):1736–41. <https://doi.org/10.1210/en.2002-220013>.
 31. Cragolini AB, Perelló M, Schiöth HB, Scimone TN. α -MSH and γ -MSH inhibit IL-1 β induced activation of the hypothalamic-pituitary-adrenal axis through central melanocortin receptors. *Regul Pept*. 2004;122(3):185–90. <https://doi.org/10.1016/j.regpep.2004.06.011>.
 32. Young JB, Rosa RM, Landsberg L. Dissociation of sympathetic nervous system and adrenal medullary responses. *Am J Physiol Endocrinol Metab*. 1984. <https://doi.org/10.1152/ajpendo.1984.247.1.E35>.
 33. Young JB, Landsberg L. Suppression of sympathetic nervous system during fasting. *Obes Res*. 1997;5(6):646–9. <https://doi.org/10.1002/j.1550-8528.1997.tb00590.x>.
 34. Wang M, Wang Q, Whim MD. Fasting induces a form of autonomic synaptic plasticity that prevents hypoglycemia. *Proc Natl Acad Sci USA*. 2016;113(21):E3029–38. <https://doi.org/10.1073/pnas.1517275113>.
 35. Perelló M, Gaillard RC, Chisari A, Spinedi E. Adrenal enucleation in MSG-damaged hyperleptinemic male rats transiently restores adrenal sensitivity to leptin. *Neuroendocrinology*. 2003;78(3):176–84. <https://doi.org/10.1159/000072799>.
 36. Mizuno TM, Kleopoulos SP, Bergen HT, Roberts JL, Priest CA, Mobbs CV. Hypothalamic pro-opiomelanocortin mRNA is reduced by fasting in ob/ob and db/db mice, but is stimulated by leptin. *Diabetes*. 1998;47(2):294–7. <https://doi.org/10.2337/diab.47.2.294>.
 37. Williams KW, Margatho LO, Lee CE, Choi M, Lee S, Scott MM, et al. Segregation of acute leptin and insulin effects in distinct populations of arcuate proopiomelanocortin neurons. *J Neurosci*. 2010;30(7):2472–9. <https://doi.org/10.1523/JNEUROSCI.3118-09.2010>.
 38. Padilla SL, Carmody JS, Zeltser LM. Pomc-expressing progenitors give rise to antagonistic neuronal populations in hypothalamic feeding circuits. *Nat Med*. 2010;16(4):403–5. <https://doi.org/10.1038/nm.2126>.
 39. Lam BYH, Cimino I, Poles-Wolf J, Nicole Kohnke S, Rimmington D, Iyemere V, et al. Heterogeneity of hypothalamic pro-opiomelanocortin-expressing neurons revealed by single-cell RNA sequencing. *Mol Metab*. 2017;6(5):383–92. <https://doi.org/10.1016/j.molmet.2017.02.007>.
 40. Bell BB, Harlan SM, Morgan DA, Guo DF, Rahmouni K. Differential contribution of POMC and AgRP neurons to the regulation of regional autonomic nerve activity by leptin. *Mol Metab*. 2018;8:1–12. <https://doi.org/10.1016/j.molmet.2017.12.006>.
 41. Caron A, Lemko HMD, Castorena CM, Fujikawa T, Lee S, Lord CC, et al. POMC neurons expressing leptin receptors coordinate metabolic responses to fasting via suppression of leptin levels. *Elife*. 2018;7:e38704. <https://doi.org/10.7554/eLife.33710>.
 42. Ünler AG, Keçik O, Quaresma PGF, De Araujo TM, Lee H, Li W, et al. Role of POMC and AgRP neuronal activities on glycaemia in mice. *Sci Rep*. 2019. <https://doi.org/10.1038/s41598-019-49295-7>.
 43. Zhan C, Zhou J, Feng Q, Zhang J, Lin S, Bao J, et al. Acute and long-term suppression of feeding behavior by POMC neurons in the brainstem and hypothalamus, respectively. *J Neurosci*. 2013;33(8):3624–32. <https://doi.org/10.1523/JNEUROSCI.2742-12.2013>.
 44. Dodd GT, Michael NJ, Lee-Young RS, Mangiafico SP, Pryor JT, Munder AC, et al. Insulin regulates POMC neuronal plasticity to control glucose metabolism. *Elife*. 2018;7:e38704. <https://doi.org/10.7554/eLife.38704>.
 45. Steculorum SM, Ruud J, Karakasilioti I, Backes H, Engström Ruud L, Timper K, et al. AgRP neurons control systemic insulin sensitivity via myostatin expression in brown adipose tissue. *Cell*. 2016;165(1):125–38. <https://doi.org/10.1016/j.cell.2016.02.044>.
 46. Krashes MJ, Shah BP, Madara JC, Olson DP, Strohlic DE, Garfield AS, et al. An excitatory paraventricular nucleus to AgRP neuron circuit that drives hunger. *Nature*. 2014;507(7491):238–42. <https://doi.org/10.1038/nature12956>.
 47. Aponte Y, Atasoy D, Sternson SM. AGRP neurons are sufficient to orchestrate feeding behavior rapidly and without training. *Nat Neurosci*. 2011;14(3):351–5. <https://doi.org/10.1038/nn.2739>.
 48. Betley JN, Cao ZFH, Ritolola KD, Sternson SM. Parallel, redundant circuit organization for homeostatic control of feeding behavior. *Cell*. 2013. <https://doi.org/10.1016/j.cell.2013.11.002>.
 49. Parker SL, Balasubramaniam A. Neuropeptide Y Y2 receptor in health and disease. *Br J Pharmacol*. 2008. <https://doi.org/10.1038/sj.bjp.0707445>.
 50. Kim JS, Kim WB, Kim YB, Lee Y, Kim YS, Shen FY, et al. Chronic hyperosmotic stress converts GABAergic inhibition into excitation in vasopressin and oxytocin neurons in the rat. *J Neurosci*. 2011;31(37):13312–22. <https://doi.org/10.1523/JNEUROSCI.1440-11.2011>.
 51. Kim YB, Kim WB, Kim WB, Shen FY, Lee SW, Chung HJ, et al. GABAergic excitation of vasopressin neurons: possible mechanism underlying sodium-dependent hypertension. *Circ Res*. 2013;113(12):1296–307. <https://doi.org/10.1161/CIRCRESAHA.113.301814>.
 52. Kakizawa K, Watanabe M, Mutoh H, Okawa Y, Yamashita M, Yanagawa Y, et al. A novel GABA-mediated corticotropin-releasing hormone secretory mechanism in the median eminence. *Sci Adv*. 2016;2(8):e1501723. <https://doi.org/10.1126/sciadv.1501723>.
 53. Vella KR, Ramadoss P, Lam FS, Harris JC, Ye FD, Same PD, et al. NPY and MC4R signaling regulate thyroid hormone levels during fasting through both central and peripheral pathways. *Cell Metab*. 2011;14(6):780–90. <https://doi.org/10.1016/j.cmet.2011.10.009>.
 54. Dietrich MO, Zimmer MR, Bober J, Horvath TL. Hypothalamic AgRP neurons drive stereotypic behaviors beyond feeding. *Cell*. 2015;160(6):1222–32. <https://doi.org/10.1016/j.cell.2015.02.024>.
 55. Volpi S, Rabadan-Diehl C, Aguilera G. Vasopressinergic regulation of the hypothalamic pituitary adrenal axis and stress adaptation. *Stress*. 2004;7(2):75–83. <https://doi.org/10.1080/10253890410001733535>.
 56. Ulrich-Lai YM, Engeland WC. Sympatho-adrenal activity and hypothalamic-pituitary-adrenal axis regulation. In *Techniques in the Behavioral and Neural Sciences*, Vol. 15, Part 1. Amsterdam: Elsevier; 2005. [https://doi.org/10.1016/S0921-0709\(05\)80024-0](https://doi.org/10.1016/S0921-0709(05)80024-0).
 57. Lolait SJ, Stewart LQ, Jessop DS, Young WS III, O'Carroll AM. The hypothalamic-pituitary-adrenal axis response to stress in mice lacking functional vasopressin V1b receptors. *Endocrinology*. 2007;148(2):849–56. <https://doi.org/10.1210/en.2006-1309>.
 58. Stanley S, Pinto S, Segal J, Pérez CA, Viale A, DeFalco J, et al. Identification of neuronal subpopulations that project from hypothalamus to both liver and adipose tissue polysynaptically. *Proc Acad Sci USA*. 2010;107(15):7024–9. <https://doi.org/10.1073/pnas.1002790107>.
 59. Pralong FP, Roduit R, Waeber G, Castillo E, Mosimann F, Thorens B, et al. Leptin inhibits directly glucocorticoid secretion by normal human and rat adrenal gland. *Endocrinology*. 1998;139(10):4264–8. <https://doi.org/10.1210/endo.139.10.6254>.
 60. Harris HJ, Kotelevtsev Y, Mullins JJ, Seckl JR, Holmes MC. Intracellular regeneration of glucocorticoids by 11 β -hydroxysteroid dehydrogenase (11 β -HSD)-1 plays a key role in regulation of the hypothalamic-pituitary-adrenal axis: Analysis of 11 β -HSD-1-deficient mice. *Endocrinology*. 2001;142(1):114–20. <https://doi.org/10.1210/endo.142.1.7887>.
 61. Paterson JM, Holmes MC, Kenyon CJ, Carter R, Mullins JJ, Seckl JR. Liver-selective transgene rescue of hypothalamic-pituitary-adrenal axis dysfunction in 11 β -hydroxysteroid dehydrogenase type 1-deficient mice. *Endocrinology*. 2007;148(3):961–6. <https://doi.org/10.1210/en.2006-0603>.
 62. Balthasar N, Coppari R, McMinn J, Liu SM, Lee CE, Tang V, et al. Leptin receptor signaling in POMC neurons is required for normal body weight homeostasis. *Neuron*. 2004;42(6):983–91. <https://doi.org/10.1016/j.neuron.2004.06.004>.
 63. Tong Q, Ye CP, Jones JE, Elmquist JK, Lowell BB. Synaptic release of GABA by AgRP neurons is required for normal regulation of energy balance. *Nat Neurosci*. 2008;11(9):998–1000. <https://doi.org/10.1038/nn.2167>.
 64. Krashes MJ, Koda S, Ye C, Rogan SC, Adams AC, Cusher DS, et al. Rapid, reversible activation of AgRP neurons drives feeding behavior in mice. *J Clin Invest*. 2011;121(4):1424–8. <https://doi.org/10.1172/JCI46229>.
 65. Cabral A, Fernandez G, Tolosa MJ, Rey Moggia A, Calfa G, De Francesco PN, et al. Fasting induces remodeling of the orexigenic projections from the arcuate nucleus to the hypothalamic paraventricular nucleus, in a growth hormone secretagogue receptor-dependent manner. *Mol Metab*. 2020;32:69–84. <https://doi.org/10.1016/j.molmet.2019.11.014>.
 66. Cabral A, Suescun O, Zigman JM, Perello M. Ghrelin indirectly activates hypophysiotropic CRF neurons in rodents. *PLoS ONE*. 2012;7(2):e31462. <https://doi.org/10.1371/journal.pone.0031462>.

67. Schindelin J, Arganda-Carreras I, Frise E, Kaynig V, Longair M, Pietzsch T, et al. Fiji: an open-source platform for biological-image analysis. *Nat Methods*. 2012;9(7):676–82. <https://doi.org/10.1038/nmeth.2019>.
68. Franklin K, Paxinos G. the mouse brain in stereotaxic coordinates, compact. 3rd ed. London: Academic Press; 2008. <https://www.elsevier.com/books/the-mouse-brain-in-stereotaxic-coordinates-compact/franklin/978-0-12-374244-5>.
69. Rorato R, Reis WL, Antunes-Rodrigues J, Elias LL. Cholecystokinin and hypothalamic corticotrophin-releasing factor participate in endotoxin-induced hypophagia. *Exp Physiol*. 2011;96(4):439–50. <https://doi.org/10.1113/expphysiol.2010.056465>.

Publisher's Note

Springer Nature remains neutral with regard to jurisdictional claims in published maps and institutional affiliations.

Ready to submit your research? Choose BMC and benefit from:

- fast, convenient online submission
- thorough peer review by experienced researchers in your field
- rapid publication on acceptance
- support for research data, including large and complex data types
- gold Open Access which fosters wider collaboration and increased citations
- maximum visibility for your research: over 100M website views per year

At BMC, research is always in progress.

Learn more biomedcentral.com/submissions

